Beta Oscillations Relate to the N400m During Language Comprehension

Lin Wang,[1,2,3] Ole Jensen,[2] Danielle van den Brink,[2] Nienke Weder,[2] Jan-Mathijs Schoffelen,[2] Lilla Magyari,[1] Peter Hagoort,[1,2] and Marcel Bastiaansen[1,2]*

[1]*Max Planck Institute for Psycholinguistics, Nijmegen, The Netherlands*
[2]*Donders Institute for Brain, Cognition and Behaviour, Centre for Cognitive Neuroimaging, Radboud University Nijmegen, The Netherlands*
[3]*Institute of Psychology, Chinese Academy of Sciences, Beijing, China*

Abstract: The relationship between the evoked responses (ERPs/ERFs) and the event-related changes in EEG/MEG power that can be observed during sentence-level language comprehension is as yet unclear. This study addresses a possible relationship between MEG power changes and the N400m component of the event-related field. Whole-head MEG was recorded while subjects listened to spoken sentences with incongruent (IC) or congruent (C) sentence endings. A clear N400m was observed over the left hemisphere, and was larger for the IC sentences than for the C sentences. A time–frequency analysis of power revealed a decrease in alpha and beta power over the left hemisphere in roughly the same time range as the N400m for the IC relative to the C condition. A linear regression analysis revealed a positive linear relationship between N400m and beta power for the IC condition, not for the C condition. No such linear relation was found between N400m and alpha power for either condition. The sources of the beta decrease were estimated in the LIFG, a region known to be involved in semantic unification operations. One source of the N400m was estimated in the left superior temporal region, which has been related to lexical retrieval. We interpret our data within a framework in which beta oscillations are inversely related to the engagement of task-relevant brain networks. The source reconstructions of the beta power suppression and the N400m effect support the notion of a dynamic communication between the LIFG and the left superior temporal region during language comprehension. *Hum Brain Mapp 33:2898–2912, 2012.* © 2012 Wiley Periodicals, Inc.

Key words: language comprehension; semantic violation; MEG; ERF; N400m; beta oscillations

INTRODUCTION

It is generally agreed that during language comprehension, incoming sounds or orthographic patterns that correspond to individual words, trigger a cascade of memory retrieval operations that make available the necessary ingredients for understanding the message. Subsequently, these different ingredients, which include the phonologic, syntactic and semantic properties of words, have to be integrated (unified) to yield a coherent interpretation of the linguistic input. Thus, two cognitive processes play a crucial role during language comprehension: retrieval of word-level information from long-term memory, and

Additional Supporting Information may be found in the online version of this article.

*Correspondence to: Marcel Bastiaansen, Max Planck Institute for Psycholinguistics, P.O. Box 310, AH Nijmegen 6500, The Netherlands. E-mail: marcel.bastiaansen@mpi.nl

Received for publication 17 September 2010; Revised 21 June 2011; Accepted 21 June 2011

DOI: 10.1002/hbm.21410

Published online 4 April 2012 in Wiley Online Library (wileyonlinelibrary.com).

© 2012 Wiley Periodicals, Inc.

syntactic and semantic unification of this word-level information into the overall sentence (and discourse) context. Unification operations recruit the left inferior frontal gyrus [for a review see Hagoort, 2005].

The fast and dynamic neural processes underlying unification in language comprehension can be accurately measured by EEG and MEG techniques, which have a high temporal resolution. In particular, MEG is useful for localizing the sources of the recorded signals, because in contrast to EEG it does not suffer from the spatial smearing effects due to the poor conductivity of skull. Therefore, we use MEG in this study to investigate the neuronal dynamics underlying language. More specifically, we were interested in the relationship between the event-related fields (ERFs), derived from averaging MEG signals across multiple trials, and oscillatory dynamics, derived through time–frequency transformation of the MEG signals.

ERFs have been extensively explored in psycholinguistic research. For example, the N400m was found to be sensitive to semantic violations [Halgren et al., 2002; Helenius et al., 1998; Salmelin et al., 1996]. However, the ERF only represents phase-locked neural activity in MEG recordings, therewith ignoring non-phase-locked activity, as this is largely cancelled due to the averaging procedure [for discussion, see Makeig et al., 2004; Tallon-Baudry and Bertrand, 1999].

Non-phase-locked activity is most notably expressed by event-related changes in power and coherence of neuronal oscillations. Oscillations in specific frequency bands have often been implicated in a wide variety of cognitive functions, such as visual binding, attention, working memory, long-term memory and more [see Klimesch and Neuper, 2006 for reviews]. However, because of space constraints, we will only briefly discuss the literature relating neuronal oscillations to language comprehension processes. Different aspects of language comprehension have been linked to oscillatory dynamics in different frequency ranges [for reviews, see Bastiaansen and Hagoort, 2006; Weiss and Mueller, 2003]. For instance, lexical retrieval has been related to theta (around 5 Hz) and alpha (around 10 Hz) frequency bands [Bastiaansen et al., 2005, 2008; Rohm et al., 2001]. Semantic unification, in contrast, has been related to changes in gamma (above 30 Hz) oscillations [Braeutigam et al., 2001; Hagoort et al., 2004; Hald et al., 2006]. Finally, syntactic unification has been tentatively linked to reactivity in the beta frequency band [Bastiaansen et al., 2006, 2009; Davidson and Indefrey, 2007; Weiss et al., 2005]. Nevertheless, other findings also point to a broader role for β-band activity within the domain of language processing. For instance, larger beta power suppression has been reported for open-class words versus closed-class words [Bastiaansen et al., 2005], for emotional versus neutral words [Hirata et al., 2007], for deviant syllables versus standard syllables in an oddball paradigm [Kim and Chung, 2008], for listening to words versus pseudo-words [Supp et al., 2004], for naming/perceiving incongruent versus congruent color words during the Stroop task [Liu et al., 2006; Schack et al., 1999] and during a word generation task [Yamamoto et al., 2006]. To summarize, the available data concerning beta oscillations and language comprehension shows a rather diverse picture.

Different views have been expressed concerning the relationship between event-related responses and oscillatory activity. One view is that the ERPs/ERFs are generated by additive evoked responses, which are fully independent of ongoing oscillations [Mäkinen et al., 2005; Shah et al., 2004]. A diametrically opposing view is that ERPs/ERFs exclusively emerge from the phase resetting of ongoing oscillations [Hanslmayr et al., 2007; Makeig et al., 2002]. It is however possible to envisage an "in-between" position, where oscillatory activity influences, but not fully determines ERP/ERF amplitudes [Intriligator and Polich, 1994; Jasiukaitis and Hakerem, 1988; Mathewson et al., 2009; Mazaheri and Picton, 2005]. For instance, Mazaheri and Jensen [2008] recently demonstrated that the slow evoked components in ERPs/ERFs can be generated by the asymmetric modulation of peaks and troughs of the ongoing oscillatory brain activities. This is an instance of a mechanism in which some aspects of the ERP/ERF are modulated and/or generated through aspects of the ongoing oscillatory activity. In sum, the exact relation between event-related changes in oscillatory activity on the one hand, and evoked activity (i.e., ERPs/ERFs) on the other hand, is rather complex and merits further investigation.

To further characterize the role of oscillatory brain activity in language comprehension, we recorded the ongoing MEG from subjects listening to sentences in which the final word was either semantically congruent or incongruent with the preceding sentence context. We are particularly interested in whether a relationship exists between MEG oscillatory dynamics (notably power changes) and the N400m. We therefore present detailed analyses of both the event-related fields (ERFs) and the time–frequency representations (TFRs) of power changes, and explicitly investigate possible relationships between these two dependent measures.

METHODS

Subjects

Ten healthy native speakers of Dutch (ages 18–25, five males, right handed) participated in the experiment. None of them had a history of neurological disorders. Informed consent was obtained from each subject according to the declaration of Helsinki.

Materials

We used the same set of materials as in the event-related potentials (ERP) study of van den Brink et al. [2001]. Three types of sentences were constructed. In the congruent condition (C), the sentences ended with a high-cloze probability word (average cloze probability: 0.84; range: 0.5–1.0), e.g., De klimmers bereikten eindelijk de

top van de berg. (The climbers finally reached the top of the mountain.). In the incongruent condition (IC), sentences ended with a semantically anomalous word, which was unexpected given the sentential context, e.g., De klimmers bereikten eindelijk de top van de tulp. (The climbers finally reached the top of the tulip.). The third type of sentences ended with a semantically anomalous word that had the same initial phonemes (and lexical stress) as the high-cloze words from the congruent condition. This condition was introduced for reasons not relevant to this paper. Since we only are interested in comparing IC with C, we will not report the data for this condition.

A set of 261 triplets of sentences were constructed for the three experimental conditions. The sentences in each triplet were identical up to the final word. The critical sentence-final words in the C and IC conditions were matched on frequency and duration, with average log frequencies of 2.87 versus 2.49 [Baayen et al., 1993], and mean durations of 516 ms versus 515 ms for the C and IC conditions, respectively. All the sentences were spoken in a sound-attenuating booth and recorded on a digital audiotape with a sampling rate of 16 kHz. No specific voice changes marked the sentence-final anomalies as odd in the anomalous conditions (based on our subjective judgement).

Three lists (87 per condition per list) were constructed to ensure that no subject heard the same sentence or critical word more than once, and that all the sentences were presented across the three lists. In addition, a set of 87 correct filler sentences were added to each list to balance the sentences that ended congruently and anomalously. To familiarize the subjects with the experimental situation, each list was preceded by a practice list of 20 sentences reflecting the experimental materials.

Procedure

Subjects were tested individually in a dimly illuminated, sound-attenuating booth. The light level was ~10 Lumen. The subjects were seated in a relaxed position under the MEG helmet. Their task was to listen attentively to the sentences and try to understand them. They were informed that some of the sentences would be semantically anomalous. Acoustic transducers from Etymotic Research (ER-3A) were applied to present the auditory stimuli.

A trial started with a 300 ms warning tone, followed by 1,200 ms of silence. Then a sentence was presented auditorily. The next trial began 4,100 ms after sentence offset. To reduce eye blinks in the time interval in which the sentence was presented, subjects were instructed to fixate on an asterisk presented visually 1,000 ms before the beginning of the sentence. The asterisk remained on the screen until 1,600 ms after the offset of the spoken sentence. Subjects were encouraged to blink when the asterisk was not displayed on the screen.

Data Acquisition

MEG signals were recorded with 151 axial gradiometers CTF Omega System. In addition, the horizontal and vertical electrooculogram (EOG) were recorded to later discard trials contaminated by eye movements and blinks. The ongoing MEG and EOG signals were lowpass filtered at 100 Hz, digitized at 300 Hz and stored for off-line analysis. To measure the head position with respect to the axial gradiometers, three coils were placed at anatomical landmarks of the head (nasion, left and right ear canal). Although the subjects were seated under the MEG helmet, the positions of the coils were determined before and after the experiment by measuring the magnetic signals produced by currents passed through the coils.

Magnetic resonance images (MRIs) were obtained with a 1.5 T Siemens system with markers attached in the same position as the head coils. The MRIs were aligned to the MEG coordinate system according to the anatomical landmarks.

Data Preprocessing

Data were analyzed using the Fieldtrip software package, a open-source Matlab toolbox for neurophysiological data analysis [Oostenveld et al., 2011]. First the [1]MEG data were segmented into trials starting 1 s before and ending 2 s after the onset of the critical words. Then the artifacts of these trials were detected based on visual inspection by an experienced MEG researcher, without using any fixed rejection thresholds. Trials contaminated with jump artifacts, eye movements, and/or muscle activities were discarded from further analysis. Jump artifacts refer to the fact that in MEG measurements, due to the high sensitivity of the recording devices, electromagnetic disturbances in the environment can sometimes cause very brisk, and relatively large changes in the recorded signals. In the end, on average 88% of trials were kept, with equal numbers of trials per conditions [$t_{(9)} = 2.11$, $P > 0.05$].

Event-Related Field Analysis

For each subject, the ERFs of IC and C conditions were obtained by averaging the trials separately for each condition, with a baseline correction between −200 ms and 0. Besides calculating the ERFs on the data from the axial gradiometers, we also used an approximation of the planar gradient[1] to get a better topographical description of the ERFs. The planar gradient simplifies the interpretation of the sensor-level data since the neuronal sources of the signals typically are situated directly below where the planar gradient is strongest [Hämäläinen et al., 1993].

[1]Whenever we refer to sensors, or planar gradients, throughout the text, we are in fact referring to the planar gradients that are estimated from the axial gradiometer recordings. For the recordings from the axial gradiometers, we use the term axial gradiometers.

Another advantage is that we can now calculate the activation produced in a contiguous set of sensors, necessary for the cluster-randomization algorithm described later. We used the signals recorded from the axial gradiometer and the neighboring axial gradiometers (closer than 4 cm, typically six axial gradiometers) to get the planar gradient estimates for each sensor [see Bastiaansen and Knosche, 2000]. Then the estimated horizontal and vertical components of the planar gradient were combined using the root mean square $\sqrt{(\frac{dF}{dx})^2 + (\frac{dF}{dy})^2}$ resulting in positive values.

To compare the difference between the two conditions, we performed a cluster-based random permutation test (see Statistical Analyses) on the sensor level. This test increases the sensitivity of the statistics while controlling for multiple comparisons. On the basis of both visual inspection to the ERFs and the a priori knowledge that the N400m peaks around 400 ms, we selected a time interval of 200–700 ms for quantifying the ERFs. The averaged values of planar gradient within this time interval entered the statistical analyses.

Time–Frequency Representation Analysis

The TFR of the single trials were calculated using a Wavelet technique [Sinkkonen et al., 1995; Tallon-Baudry et al., 1996]. The power $E(t, f_0)$ for a given signal at time (t) and frequency (f_0) is given by the squared norm of the convolution of a Morlet wavelet, $w(t, f_0) = A \exp(-t^2/2\sigma_t^2) \exp(2i\pi f_0 t)$ to the signal $s(t)$: $E(t, f_0) = |w(t, f_0) \times s(t)|^2$, where $\sigma_t = m/2\pi f_0$, and $A = (\sigma_t \sqrt{\pi})^{-1/2}$. The constant m, which defines the compromise between time and frequency resolution, was set to 7. Therefore, the maximum length of the longest wavelet is 1,000 ms (at 7 Hz). Note that in terms of temporal resolution, wavelet transforms introduce a temporal smearing effect. In fact, any given time point in the resulting TFR is a weighted average of the time points ranging from a certain time window ($\frac{7}{2\times\text{frequency of interest}}$) around that time point. The TFRs were calculated at each sensor location for the vertical and horizontal planar gradient and then averaged [see Bastiaansen and Knosche, 2000 for a validation of this approach]. Subsequently, we averaged the planar gradient power estimates over trials for both conditions. The resulting power changes in the post-stimulus interval (relative to the onset of the critical word) were expressed as an absolute power change relative to the pre-stimulus interval (−600 ms to −100 ms, referring to the center of the wavelet), during which time the subjects were listening to the congruent words in the sentence.

Similar to the statistical analysis of the ERFs, we performed a cluster-based random permutation test on the sensor level to test for TFR differences. On the basis of both visual inspection and the expected alpha and beta effect from previous studies [Bastiaansen et al., 2009; Klimesch, 1999], frequency and time ranges within which the TFRs show large differences between the two conditions were selected as follows: 8–11 Hz, 200–1,200 ms for the alpha band; 16–19 Hz, 200–700 ms for the beta band. The averaged values in these ranges were then calculated. Note that due to the temporal smearing effect, the time intervals used for analysis were effectively broadened both for the alpha range (approximately −200 ms to 1,600 ms) and for the beta range (∼0 ms to ∼900 ms). However, the shape of the wavelet determines that the contribution of power in the time epochs beyond the selected time intervals to the actual wavelet output is much reduced relative to that of the power within the intervals. To reduce the large variance of power among subjects, we normalized the data of each sensor by subtracting the averaged value across all the sensors for each subject. Those values were used for further statistical tests.

Statistical Analyses

We used a cluster-based random permutation approach [Maris and Oostenveld, 2007] to test the significance of the difference between the two conditions, both for the ERFs and the TFRs. This approach controls the Type-1 error rate in a situation involving multiple comparisons. Here is a brief description of the procedure.

First, for every sensor a simple dependent-samples t test is performed. All contiguous sensors exceeding a preset significance level (5%) are grouped into clusters. For each cluster the sum of the t statistics is used in the cluster-level test statistic. Next, a null distribution which assumes no difference between conditions is created. This distribution is obtained by 1,000 times randomly assigning the conditions in subjects and calculating the largest cluster-level statistic for each randomization. Finally, the actually observed cluster-level test statistics are compared against the null distribution, and clusters falling in the highest or lowest 2.5th percentile are considered significant.

A Linear Regression Analysis Between the Oscillatory Power and the N400m in the IC and C Conditions

To characterize the relationship between power changes and N400m for both conditions, we performed a linear regression analysis between the two frequency bands (alpha and beta) that show significant power differences between the two conditions and the N400m in the post-stimulus interval, separately for the IC and C conditions.

First, the time window and frequency band were selected based on the statistical analysis results that showed significant TFR differences between the two conditions. Then in the selected time window the power modulation with respect to the pre-stimulus baseline was calculated for each individual trial, for both conditions. For each subject, after combining the two conditions, we sorted all the trials into five bins according to the power of the planar gradients in the selected frequency band at

the location of the (individually determined) sensor that showed the largest power modulation. Next, the ERF of each bin was calculated for the corresponding trials by averaging the MEG data for the C and IC conditions separately (after applying a 20 Hz low-pass filter). Then for each bin we extracted the N400m amplitudes (time interval: 200–700 ms) of the sensors that showed significant differences between the two conditions on N400 amplitudes. These values were normalized by subtracting the averaged values across the five bins, separately for each sensor and each subject. To reduce the variance of the ERFs on individual sensors, we then averaged the N400m values across the selected sensors. Then a regression analysis was performed separately for the IC and C conditions.

Source Reconstruction of N400m and Power Changes

A distributed source-modeling approach, minimum norm estimates [MNE; Dale et al., 2000; Hämäläinen and Ilmoniemi, 1994] was applied to identify the sources of the N400m differences in the two conditions. The anatomical preprocessing necessary for the source reconstruction was done as described by Dale et al. [1999] and Hämäläinen [2009], using Freesurfer (http://surfer.nmr.mgh.harvard.edu/) and MNE Suite (http://www.nmr.mgh.harvard.edu/martinos/userInfo/data/sofMNE.php).

For the source reconstruction of N400m, we used artifact-free, axial gradiometers data of the ERF analysis. Subject-averages of the two conditions were obtained with a baseline correction between −150 and 0 ms and with a low-pass filter of 35 Hz. The noise-covariance at each axial gradiometer was also estimated for each subject in each condition by estimating the noise-covariance of each trial between −1,000 and 0 ms and then by averaging the noise-covariance estimate across trials. The MNE source-analysis was performed based on the leadfield, the ERF average and noise-covariance estimate for each subject for each condition. The grid resolution was 3.9 mm^2. After that the power values of the source-estimates were averaged between 200 and 700 ms after stimulus onset, and the difference of the averaged power values of the two conditions (IC–C) were calculated, downsampled and spatially normalized to a template MRI. At the end, the normalized power values of the difference of the conditions were averaged over subjects.

To identify the sources in the beta band for the C and IC conditions, we used a beamforming approach, Dynamic Imaging of Coherent Sources [DICS; Gross et al., 2001]. Based on the TFRs from the sensor level analysis, a Hanning window was applied to a 0.5 s time window (200–700 ms), which resulted in a frequency smoothing of ~3 Hz. Following a FFT, the spectral values at 18 Hz were extracted (with the frequency range around 16.5–19.5 Hz).

The source reconstruction of power changes was done based on the data from axial gradiometers. First, a semi-realistic head model developed by Nolte [2003] was constructed. It is based on a correction of the lead field for a spherical volume conductor by a superposition of basis functions, gradients of harmonic functions constructed from spherical harmonics. Then the brain volume of each subject was divided into a grid with 1 cm resolution, and the lead field was calculated for each grid point. After that, a spatial filter was constructed for each grid point by using the lead field and the cross-spectral density. In the end, the power at each grid point for both conditions was estimated by applying the filter to the Fourier transformed data. In this study, a common filter was built for the two conditions, and the difference in power between conditions was estimated by $(Source_{IC}–Source_{C})/(Source_{IC} + Source_{C})$. Before averaging the source estimates over subjects, we spatially normalized the data to the MNI brain according to the individual brain shapes [Montreal Neurological Institute (MNI), Montreal, Quebec, Canada; http://www.bic.mni.mcgill.ca/brainweb].

RESULTS

The IC Condition Elicits a Larger N400m than the C Condition

To confirm previous findings on the effect of semantic anomaly, we compared the ERFs of the two conditions. Figure 1A shows the planar gradient of the ERFs time-locked to the onset of the critical words averaged over 10 subjects. Approximately between 200 ms and 700 ms after the critical words, the IC condition elicited larger amplitudes than the C condition over bilateral, left-hemisphere-dominant temporal areas. Our data are compatible with previously reported ERF equivalents of the N400 ERP [the N400m; Halgren et al., 2002; Helenius et al., 1998, 2002; Salmelin et al., 1996]. Figure 1B displays the grand average of the ERF topographies in the time interval between 200 and 700 ms of the axial gradient. Except for the C condition, both the IC condition and the subtraction (IC–C) showed a strong dipolar pattern over the left hemisphere, and a weaker dipolar pattern over the right hemisphere. In addition, Figure 1C presents the topographies of the planar gradient fields. The left lateralization of the N400m component was confirmed for both the IC condition and the subtraction (IC–C). The contrast between IC and C revealed a significant cluster ($P = 0.03$) over the left temporal area (the sensors of this cluster are marked in Fig. 1C).

The stimulus set applied in this study has also been used in an ERP study by van den Brink et al. [2001]. The time course and topography of the ERPs are shown in Figure 1D,E. The time course of the ERPs (Fig. 1D) is quite similar to those in Figure 1A with respect to the difference in waveforms, but the topography of the ERP difference (Fig. 1E) is much more spatially smeared compared to the topography of ERFs (Fig. 1C). Also, the ERP effect does not show the left lateralization.

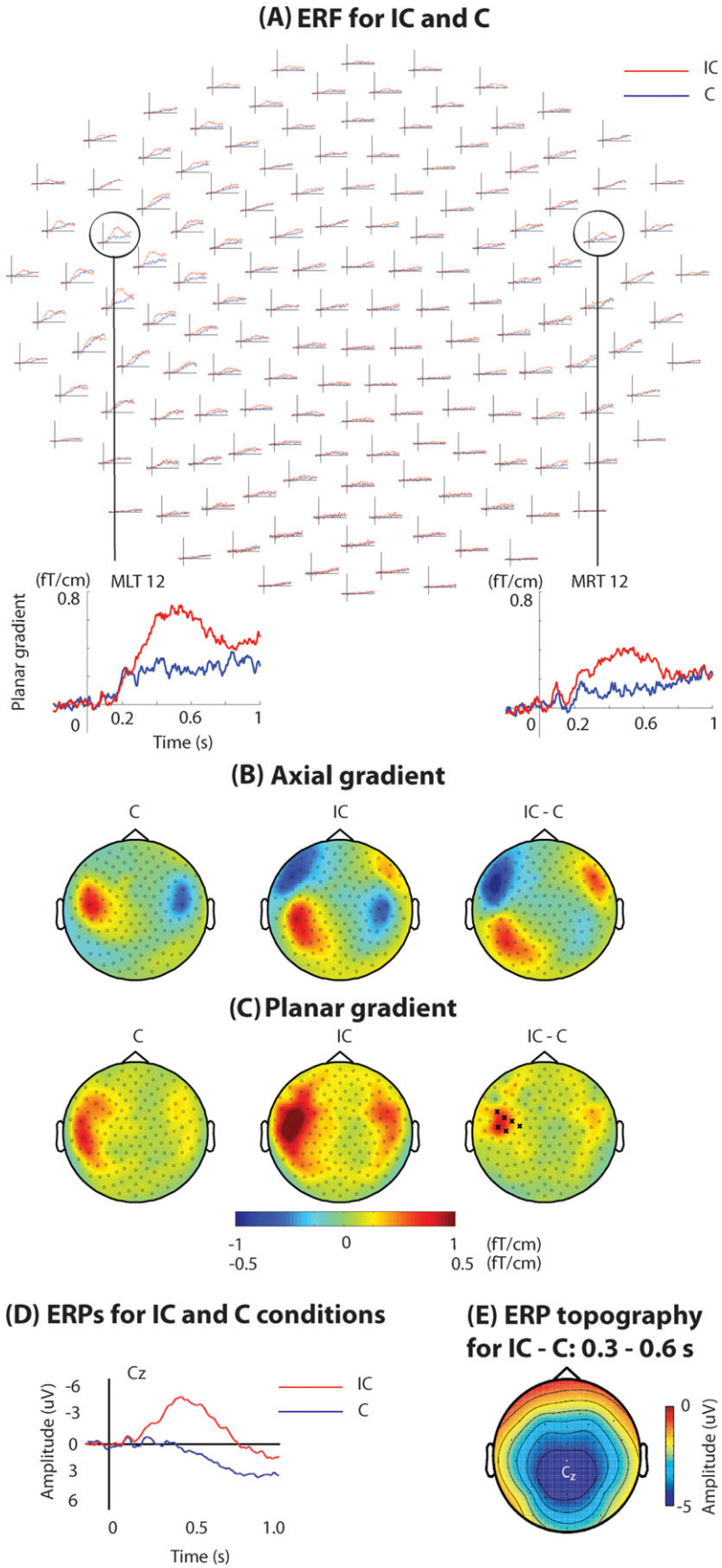
(A) ERF for IC and C
IC
C
(fT/cm)
MLT 12
0.8
Planar gradient
0
0.2
0.6
1
Time (s)
(fT/cm)
MRT 12
0.8
0
0.2
0.6
1
(B) Axial gradient
C
IC
IC - C
(C) Planar gradient
C
IC
IC - C
-1
0
1
(fT/cm)
-0.5
0.5
(fT/cm)
(D) ERPs for IC and C conditions
Cz
IC
C
Amplitude (uV)
-6
-3
0
3
6
0
0.5
1.0
Time (s)
(E) ERP topography
for IC - C: 0.3 - 0.6 s
Cz
0
-5
Amplitude (uV)

Figure 1.

The IC Condition Induces a Power Decrease Over Left Temporal Areas in Both the Alpha and Beta Frequency Bands

Figure 2A presents the grand averaged TFRs for a representative sensor MLC15 (the location of this sensor is marked by a white circle in Fig. 2B). The TFRs of all the sensors are shown in the Supporting Information figures (see Fig. S1–S3 for C, IC and IC–C, respectively). In Figure 2A, the IC condition shows a power decrease both in the alpha frequency band (8–11 Hz) and the lower beta frequency range (here 16–19 Hz), which is absent in the C condition. The strong alpha and beta power changes are also evident in the subtraction (IC–C).

The topographical distribution of the beta power changes (Fig. 2B) is similar to that of the N400m effect in the ERF analysis, especially in the 200–700 ms interval after onset of the critical word (CW). The statistical analysis of the difference between the two conditions revealed a significantly lower beta power for the IC than C condition over left temporal areas ($P = 0.04$; the sensors showing a significant effect are marked on the topography of IC–C in Fig. 2B). We also found a significant cluster over the right hemisphere ($P = 0.02$), revealing that the beta power between 200 and 700 ms is larger for the IC than for the C condition. To study the time course of the beta activity, we calculated topographic maps for IC–C every 200 ms (Fig. 3A). Beta activity (16–19 Hz) starts to decrease from 200 ms after CW onset over the left hemisphere. This suppression was sustained until 1,400 ms after CW onset. Meanwhile, there was a beta increase over the right hemisphere that gradually expanded to posterior areas with a similar time course as the beta decrease.

In addition to the beta power changes, Figure 2A also shows differential alpha power (8–11 Hz) changes for the two conditions (C and IC condition). We therefore also tested the alpha power differences (8–11 Hz) in the time range 200–700 ms after CW onset. Statistical analysis showed no significant cluster in this time window ($P = 0.27$). Based on a visual inspection of alpha power difference in Figure 2A, however, a longer time window of 200–1,200 ms was selected. Statistical analysis revealed a significantly lower alpha power for the IC than C condition over left temporal-frontal area ($P = 0.04$; the significant sensors are marked on the topography of IC–C in Fig. 2C). The alpha power time course is shown in Figure 3B. Starting from 200 ms and lasting until 1,400 ms, alpha power decreased over left temporal areas, but concurrently increased over the posterior area.

Beta Power, but not Alpha Power, is Linearly Related to N400m Amplitude

Since the statistical analysis revealed significant TFR differences between the two conditions in both the beta (16–19 Hz, 200–700 ms) and alpha (8–11 Hz, 200–1,200 ms) frequency bands, the linear regression analysis was performed between respectively the beta and alpha power and the N400m in the post-stimulus interval.

For the linear regression analysis between the beta power and the N400m, the trials were sorted into five bins according to the beta power (16–19 Hz, 200–700 ms) measured on the MEG sensors that showed the largest beta power difference for each subject. Then the N400m amplitudes (time window: 200–700 ms) of each condition were extracted from the six sensors that showed significant N400m differences between the two conditions (indicated in Fig. 1C). Note that different sets of sensors were used to quantify the N400m and the beta/alpha power changes, in order to optimize the signal-to-noise ratio in these measures.

The linear regression analysis revealed a positive linear regression between N400m and beta power ($R = 0.30$, $P = 0.03$) for the IC condition (Fig. 4A), while no significant regression was found for the C condition ($P = 0.64$, see Fig. 4B).

Similarly, the alpha power (8–11 Hz, 200–1,200 ms) at the location of the sensors that showed the largest alpha modulation was taken into account to group the trials into five bins. And the N400m amplitudes (time window: 200–700 ms) of the six sensors (indicated in Fig. 1C) were used for further regression analysis. We found no significant regression (Fig. 4C,D) between N400m and the five bins of alpha modulation for either the IC condition ($P = 0.85$) or the C condition ($P = 0.90$).

The Source of the N400m and the Beta Power Decrease are Estimated to be in Superior Temporal Regions and Broca's Area, Respectively

By using minimum norm estimates, the source of the N400m effect (time window 200–700 ms after CW onset) was estimated to be in the left superior temporal region,

Figure 1. Results of the ERF analysis and the ERPs obtained from a previous EEG study using the same stimulus set as used in the current study. (**A**) Grand average ERFs for the congruent (C) and incongruent (IC) conditions for all sensors, with insets for two representative sensors. The IC condition shows a larger N400m than the C condition. (**B**) Topographies of the ERFs (axial gradient) in the time window of 200–700 ms for the C, IC, and IC–C. Both the IC condition and the subtraction (IC–C) show a strong dipolar pattern over the left hemisphere and a weaker dipolar pattern over the right hemisphere. (**C**) Similar topographies of the three conditions (C, IC, IC–C), of the planar gradient ERFs. The sensors that show significant N400m differences between the IC and C conditions are marked "x" on the topographic plots of IC–C. (**D**) ERPs for the congruent (C, blue) and incongruent (IC, red) conditions for a representative electrode Cz. The IC condition elicited a larger N400 than the C condition. (**E**) The topography of the ERP difference (IC–C) within the time window of 300–600 ms. The data were obtained from van den Brink et al. (2001).

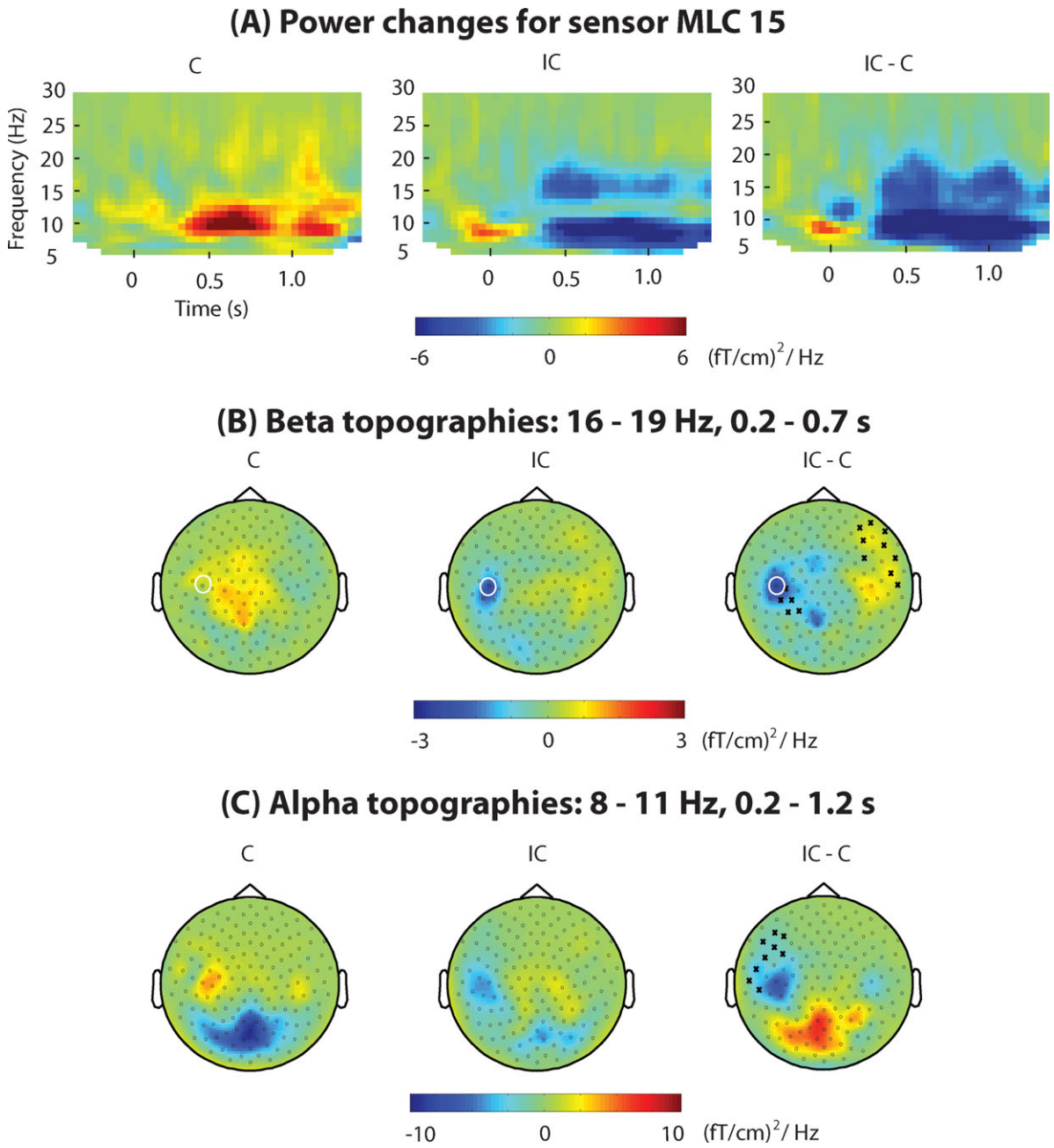

Figure 2.

Results of the time–frequency (TF) analysis. (**A**) Power changes following the critical words in the congruent (C), incongruent (IC), and the difference (IC–C) conditions for a representative sensor MLC 15 (see Fig. 2B for the location of the sensor). (**B**) Topographies of the beta power (16–19 Hz) in the time interval of 200–700 ms. The sensors that show significant differences between the IC and C conditions are marked by "x" on the IC–C topographical map. The selected sensor for displaying the power changes in Figure 2A is marked with a white circle. (**C**) Topographies of the alpha power (8–11 Hz) in the time window of 200−1,200 ms. The sensors that show significant differences between the IC and C conditions are marked as "x" on the IC–C topographical map.

extending into middle temporal as well as inferior parietal areas. The MNI coordinates of the peak activation (−42, −18, and 8) are in superior temporal gyrus (see Fig. 5A).

The source modeling based on beamformers allowed us to estimate the generators of the beta suppression for the IC relative to C condition. Because alpha power did not

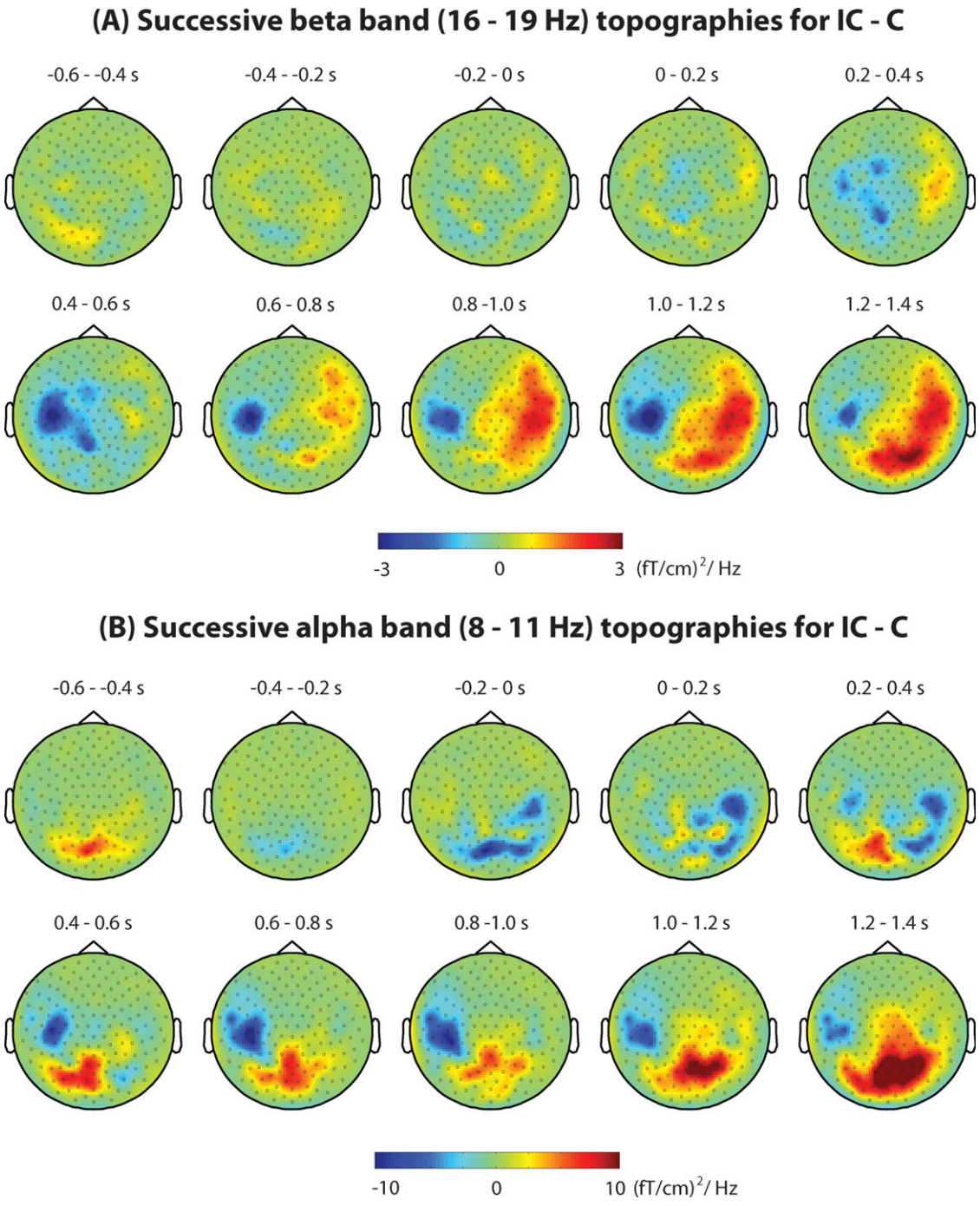

Figure 3.

Successive topographies of power changes in the beta (16–19 Hz) and alpha frequency bands (8–11 Hz) for IC–C. The time interval is between −600 ms and 1,400 ms relative to the onset of the critical words, with a time step of 200 ms. (**A**) Beta power (16–19 Hz) is initially suppressed 200 ms after onset of the critical word over the left hemisphere, and this suppression lasts until 1,400 ms. Meanwhile, there is a beta increase over the right hemisphere, which gradually expands to more posterior areas. (**B**) Alpha power (8–11 Hz) decreases over left temporal areas and concurrently increases over posterior areas between 200 ms and 1,400 ms.

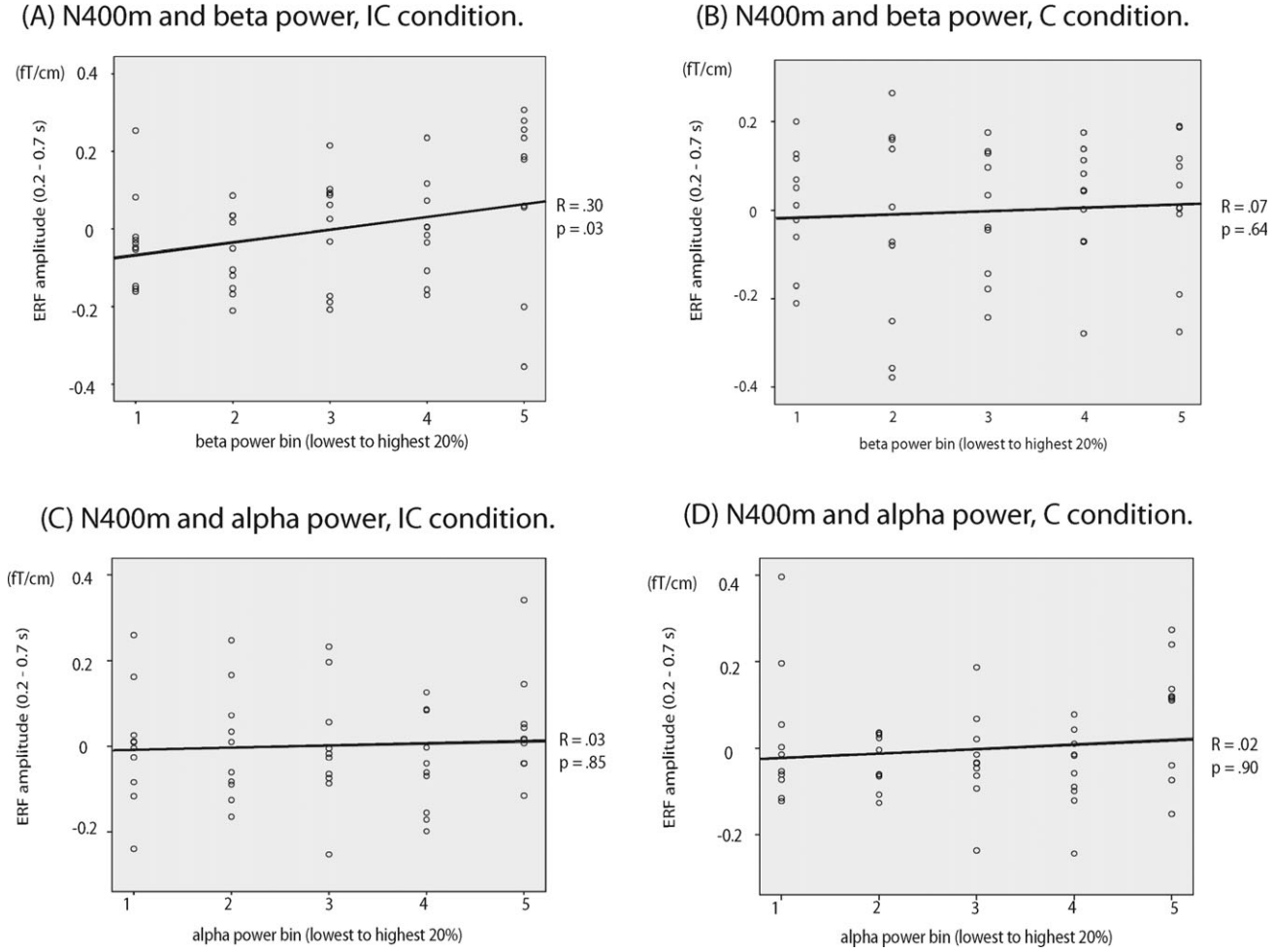

Figure 4.

(**A**) Linear regression of the N400m on beta power, for the IC condition. A significant positive relation is found between the N400m and beta power, for the IC condition. (**B**) Linear regression of the N400m on beta power, for the C condition. (**C**) Linear regression of N400m on alpha power, IC condition. (**D**) Linear regression of N400m on alpha power, C condition.

correlate with N400m amplitudes, we restricted our source modeling efforts to the observed effects in the beta range. Figure 5B shows the source of the beta suppression (time window 200–700 ms after CW onset, frequency window 16.5–19.5 Hz) for IC–C averaged over 10 subjects. The source was located in the left inferior frontal gyrus (LIFG, MNI coordinates of the peak activation: −46, 11, and −1).

DISCUSSION

MEG was used to study the neural responses engaged when subjects listen to spoken sentences with incongruent (IC) or congruent (C) sentence endings. A clear N400m was observed over the left hemisphere, and was larger for the IC sentences than for the C sentences. A time–frequency analysis of power revealed a decrease in alpha and beta power over the left hemisphere in roughly the same time range as the N400m. A linear regression analysis revealed a positive linear relationship between N400m and beta power for the IC condition, but not for the C condition. No such linear relation was found between N400m and alpha power for either condition. The sources of the beta decrease were estimated in the LIFG, and one source of the N400m was estimated in the left superior temporal region.

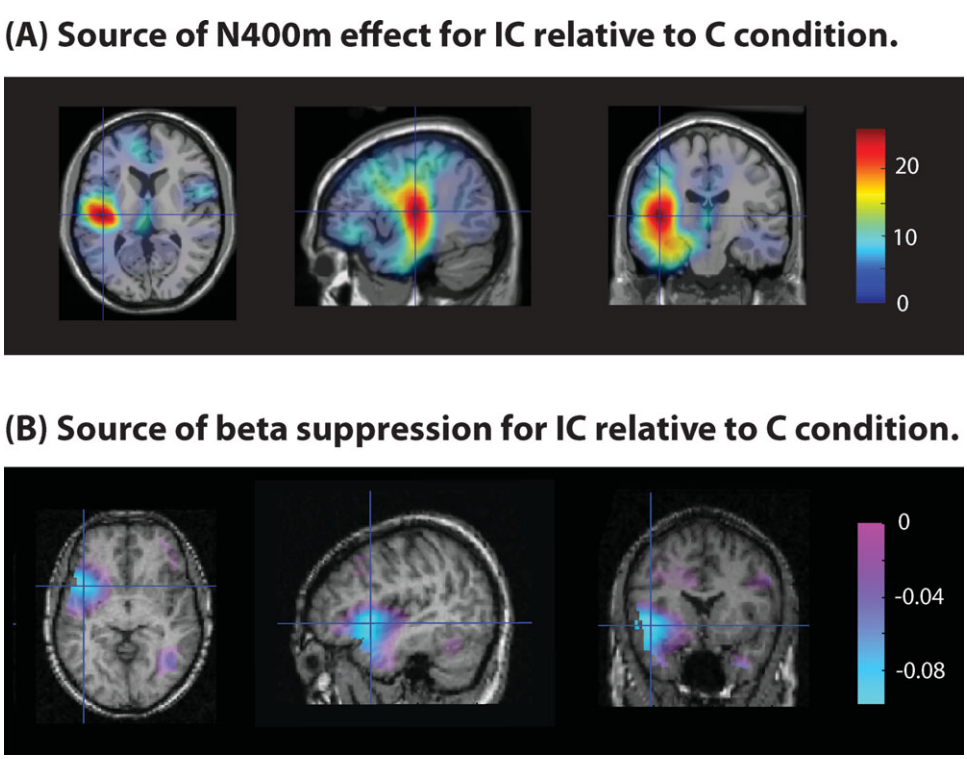

Figure 5.
(**A**) Source reconstruction of the N400m effect for the IC relative to C condition. The sources were spatially normalized to the MNI template brain. The epicentre of the source is located in the left superior temporal gyrus. (**B**) Source reconstruction of the beta power suppression for the IC relative to C condition. The sources were spatially normalized to the MNI template brain. The epicentre of the source is located in the left inferior frontal gyrus.

The Modulation of N400m Over the Left Temporal Area

The modulation of the N400m with respect to the congruency of sentences is consistent with a large number of studies [Halgren et al., 2002; Helenius et al., 1998; Salmelin et al., 1996; for a review on the EEG studies, see Kutas and Federmeier, 2000]. The N400m effect was distributed over bilateral temporal areas, with a clear left-hemisphere dominance, as shown in Figure 1C. Interestingly, the topography of the N400 effect from a previous EEG study using the same stimulus set as applied here does not show the left lateralization (Fig. 1E). Nevertheless, the topographies of the N400 effect are consistent for the EEG and MEG studies. The topography the N400 ERP effect can be explained by bilateral dipolar sources that are strongest in the left hemisphere (Fig. 1B) and oriented towards the vertex of the head. Since such dipoles produce negative potentials over the midline, no lateralization was observed in the ERP topography; however, it is observed in the ERF topography, which yields a more spatially confined activation.

The source of the N400m was estimated in the left superior temporal region and surrounding areas, which is consistent with previous MEG studies. For instance, the N400m has been reported to be generated in bilateral (but left-dominant) superior temporal regions [Halgren et al., 2002; Helenius et al., 1998; Vartiainen et al., 2009], with contributions from left prefrontal cortex in a later time window [Halgren et al., 2002]. Note however that intracranial recordings suggest that the N400 is generated in multiple brain areas, including ventrolateral prefrontal cortex, superior and middle temporal area, anterior medial temporal lobe, and hippocampus [Elger et al., 1997; Halgren et al., 1994a,b; McCarthy et al., 1995; Nobre and McCarthy, 1995]. The discrepancy might be due to the sensitivity of the employed techniques.

The Relation Between the N400 and the Alpha Power Changes

We observed consistently smaller alpha power for incongruent sentence endings as compared to congruent ones. The time window of these differential alpha power effects (roughly 200–1,200 ms after CW onset) overlaps with, but also extends over the time window of the N400m (200–700 ms after CW onset). Previous studies

have established a relation between alpha power changes and lexical retrieval [Klimesch et al., 1997a,b; Rohm et al., 2001]. Since the N400 has also been related with lexical retrieval [Lau et al., 2008], the lexical retrieval account of alpha would suggest a relationship between alpha and the N400m, but we did not find such a relationship in our data. It seems unlikely, therefore, that there exists a direct correspondence between the neural processes that are at the basis of the N400m, and those that are at the basis of the α-band effects. Rather, given the previous findings on alpha power changes in multiple cognitive tasks [for a review, see Klimesch, 1999], the differences in alpha between the conditions in the present experiment is better explained in terms of attentional differences to the critical words in the two conditions: critical words in the incongruent condition may capture more attentional resources (because of the violations they constitute are salient) than those in the congruent condition, resulting in smaller alpha power for the incongruent condition. This increased attention might not be language-specific, but a reflection of a general attention mechanism.

The Relation Between the N400m and the Beta Power Changes

In the time window of the N400m, we found a beta power decrease for the IC condition, but not for the C condition. The linear regression analysis revealed a positive regression between the N400m and the beta power for the IC condition: a larger beta power decrease in this time window was associated with smaller N400m amplitudes. Although the correlation value is not strong ($R = 0.30$), this value provides an underestimation, or at least a lower bound, of the true underlying correlation between beta oscillations and N400m, for the following two reasons. First, MEG recordings in general suffer from substantial measurement noise, which by itself would lower the observed R value to below the true underlying correlation. Second, for the regression analysis both the beta oscillations and the N400m were quantified in a small number (15 trials on average) of trials. Since both ERFs and event-related oscillations have a very low signal-to-noise ratio with such small numbers of trials, it can be expected that the observed correlation values are below the true underlying correlation.

In contrast, the C condition showed no significant linear relation between beta power and N400m in the same time interval. In addition, the source of the beta suppression for the IC relative to C condition was identified in the left inferior frontal gyrus (LIFG), an area that has been related, amongst others, to semantic unification [Bookheimer, 2002; Hagoort, 2005].

The Possible Functional Role of Beta Oscillations

As said in the introduction, beta oscillations have been related to a variety of processes involved in language comprehension, ranging from the processing of syllables, through word-level processes, to sentence-level syntactic unification. The current findings suggest an involvement of beta oscillations in semantic unification of words into the preceding sentence context. Taken together, the relationship between beta oscillations and language comprehension appears to be a complex one. However, in our opinion the different bits of data can be easily reconciled within a framework in which beta oscillations are related to the engagement of task-relevant brain regions, and in which the N400(m) relates both to semantic integration (unification) and to facilitated lexical retrieval [also discussed by Baggio and Hagoort, 2011; Kutas and Federmeier, 2011; Lau et al., 2008 for similar views]. Below we first attempt to explain the current findings using our proposed framework. Next we discuss how other findings (both inside and outside the language comprehension domain) fit in with such a framework.

In our study, the incongruent words induced a relatively strong beta power suppression after critical word onset as well as a large N400m compared with the baseline period. The source of the beta power change was estimated in the LIFG, which is consistent with results from previous studies that attempted to localize beta oscillations during language tasks [Hirata et al., 2004, 2007; Kim and Chung, 2008; Yamamoto et al., 2006]. The function of LIFG has been related with semantic unification. In the IC condition, up until the incongruent words, the brain's language system integrates the incoming information into a contextual representation without any difficulties, and the brain is well-prepared for the next congruent word(s). After encountering an incongruent word, larger efforts are needed for integrating it (or attempting to integrate it) into the preceding context. This high unification load requires a stronger engagement of the task-relevant brain network, as reflected by a larger beta power suppression in LIFG–the unification area. At the same time, lexical retrieval becomes more difficult as a result of the unexpectedness of the violating word, resulting in a large N400m. In this context, the positive correlation between beta power and N400m amplitude (i.e., stronger beta power decreases going together with smaller N400m amplitudes) might reflect an influence of unification-related processes in LIFG on retrieval-related processes in posterior superior temporal regions (where the source of the N400m was estimated). In other words, a larger engagement of unification-related areas (stronger beta decrease) yields a facilitation of the lexical retrieval process (smaller N400m). We therefore tentatively propose that the observed β-N400 correlation directly reflects the neural implementation of the facilitation of unification-guided lexical activation. Results that support this interpretation, by showing fMRI-based effective connectivity changes, are reported by Snijders et al. [2010] and by Xiang et al. [2010]. It should be noted that the proposed framework of beta suppression and network engagement can explain the data from around 200 ms onwards, but not the early evoked

responses, since the stimulus related spectral changes begin at around 200 ms.

However, the above situation only applies to the incongruent condition, where unification load is high. In the congruent condition, on the other hand, the critical words were highly predictable. Therefore, the low unification load does not require a high engagement of the LIFG, so no clear beta power suppression was induced. At the same time, lexical retrieval is relatively easy due to the high predictability of the congruent words, resulting in overall smaller N400m amplitudes relative to the IC condition, and also resulting in the absence of a β-N400m correlation.

It should be emphasized here that our current framework for interpreting beta oscillations is at odds with our previously proposed hypothesis [Bastiaansen et al., 2009] that β-band oscillations during sentence-level language comprehension reflect syntactic unification operations. However, the observation underlying this hypothesis is that sentences which contain grammatical violations produce larger beta power suppression (or smaller beta power increases, for that matter) than correct sentences [Bastiaansen et al., 2009; Davidson and Indefrey, 2007]. These observations are also consistent with the more general framework proposed here. The framework is compatible with most published findings about beta power changes during language processing. One exception is that Bastiaansen et al. [2006] reported preliminary results showing that the sentences with more complicated syntactic structure elicited larger beta power than the less complicated sentences. In this study, larger beta power was found for syntactically more complex sentences (object-relative clauses) vs. simpler ones (subject relatives). On the basis of the framework, smaller beta power would have been expected for the object-relatives, since more complex syntactic structures are expected to give rise to a stronger network engagement. However, the (preliminary) results reported by Bastiaansen et al. [2006] also stand in contrast with later reports of beta power decreases in response to syntactic violations [Bastiaansen et al., 2009, 2010]. Besides this specific issue concerning the relation between beta power changes and syntactic processing, this framework does capture a large number of other empirical observations both within and outside the domain of language comprehension. For instance, as mentioned in the introduction, the presentation of open-class words induced more beta power suppression than that of closed-class words [Bastiaansen et al., 2005]. In another interesting experiment, Sheth, Sandkühler, and Bhattacharya [2009] examined the neural activity related to solving verbal puzzles. In the period after problem presentation and before the answer, smaller beta power was found for the eventually solved versus unsolved questions.

Outside the domain of language, β-band oscillations have been reliably observed in studies using motor and somatosensory paradigms, where beta power decreases before and during the execution of movements and then rebounds after the end of the movement [Alegre et al., 2003; Kaiser et al., 2001; Pfurtscheller and Lopes da Silva, 1999; Pfurtscheller et al., 1996, 1998; Stancak and Pfurtscheller, 1996]. The sources of the sensori-motor related beta activity have been estimated to primary motor cortex [Parkes et al., 2006; Salmelin and Hämäläinen, 1995]. Finally, several studies reported beta band activity during working memory tasks. Beta band suppression was found both for working memory maintenance [Tallon-Baudry, 2003] and during information retrieval from working memory [Karrasch et al., 2004; Pesonen et al., 2006; Peterson and Thaut, 2002].

Although the aforementioned studies cover a range of cognitive functions, there is one thing that all these studies have in common: all the conditions that require more processing efforts induce more beta power suppression (but the topographical distribution of the beta power changes vary with tasks and cognitive functions). It seems then that a large body of available literature is in agreement with our proposition that beta power suppression in a given area reflects the engagement of that area in a certain task. In our opinion, this provides converging evidence for our interpretation of the present findings.

Finally, we want to emphasize that, although we report a relationship between beta oscillations and the N400m, it is important to bear in mind that this relationship might be complex or indirect. We also need to be cautious in making any assumption about the relative timing between beta oscillation and the N400m. Since there is a temporal smearing effect inherent to the time–frequency transformation that prohibits making clear statements about temporal ordering issues. Therefore, the underlying mechanism of the generation of the N400m needs to be addressed in more detail in future studies.

CONCLUSIONS

We observed a link between beta oscillations and the N400m, which provides new insights into the functional relationship between event-related oscillatory brain dynamics (i.e., beta oscillations) and event-related phase-locked MEG responses (i.e., the N400m). In addition, the source reconstructions of the beta oscillations and the N400m support the notion of a dynamic functional communication between the frontal and temporal brain areas involved in language comprehension.

REFERENCES

Alegre M, Labarga A, Gurtubay IG, Iriarte J, Malanda A, Artieda J (2003): Movement-related changes in cortical oscillatory activity in ballistic, sustained and negative movements. Exp Brain Res 148:17–25.

Baayen RH, Piepenbrock R, van Rijn H (1993): The CELEX Lexical Database (CD-ROM). Philadelphia: University of Pennsylvania.

Baggio G, Hagoort P (2011): The balance between memory and unification in semantics: Towards a dynamic account of the N400. Lang Cog Proc 26:1338–1367.

Bastiaansen M, Magyari L, Hagoort P (2009): Syntactic unification operations are reflected in oscillatory dynamics during on-line sentence comprehension. J Cogn Neurosci 22:1333–1347.

Bastiaansen M, Oostenveld R, Jensen O, Hagoort P (2008): I see what you mean: Theta power increases are involved in the retrieval of lexical semantic information. Brain Lang 106:15–28.

Bastiaansen M, Schoo LA, Hagoort P (2006): Oscillatory Neuronal Dynamics in the MEG During Syntactic Unification. 12th Annual Meeting of the Organisation for Human Brain Mapping. Florence, Italy.

Bastiaansen CM, van der Linden M, ter Keurs M, Dijkstra T, Hagoort P (2005): Theta responses are involved in lexical—Semantic retrieval during language processing. J Cogn Neurosci 7:530–541.

Bastiaansen MC, Knosche TR (2000): Tangential derivative mapping of axial MEG applied to event-related desynchronization research. Clin Neurophysiol 111:1300–1305.

Bastiaansen MCM, Hagoort P (2006): Oscillatory brain dynamics during language comprehension. In: Klimesch W, Neuper C, editors. Event-Related Dynamics of Brain Oscillations. Amsterdam, The Netherlands: Elsevier. pp 182–196.

Bookheimer S (2002): Functional MRI of language: New approaches to understanding the cortical organization of semantic processing. Annu Rev Neurosci 25:151–188.

Braeutigam S, Bailey AJ, Swithenby SJ (2001): Phase-locked gamma band responses to semantic violation stimuli. Brain Res: Cogn Brain Res 10:365–377.

Dale AM, Fischl B, Sereno MI (1999): Cortical surface-based analysis: I. Segmentation and surface reconstruction. Neuroimage 9:179–194.

Dale AM, Liu AK, Fischl BR, Buckner RL, Belliveau JW, Lewine JD, Halgren E (2000): Dynamic statistical parametric mapping: Combining fMRI and MEG for high-resolution imaging of cortical activity. Neuron 26:55–67.

Davidson DJ, Indefrey P (2007): An inverse relation between event-related and time–frequency violation responses in sentence processing. Brain Res 1158:81–92.

Elger CE, Grunwald T, Lehnertz K, Kutas M, Helmstaedter C, Brockhaus A, Van Roost D, Heinze HJ (1997): Human temporal lobe potentials in verbal learning and memory processes. Neuropsychologia 35:657–667.

Gross J, Kujala J, Hämäläinen M, Timmermann L, Schnitzler A, Salmelin R (2001): Dynamic imaging of coherent sources: Studying neural interactions in the human brain. Proc Natl Acad Sci USA 98:694–699.

Hagoort P (2005): On Broca, brain, and binding: A new framework. Trends Cogn Sci 9:416–423.

Hagoort P, Hald L, Bastiaansen MCM, Petersson KM (2004): Integration of word meaning and world knowledge in language comprehension. Science 304:438–441.

Hald LA, Bastiaansen MCM, Hagoort P (2006): EEG theta and gamma responses to semantic violations in online sentence processing. Brain Lang 96:90–105.

Halgren E, Baudena P, Heit G, Clarke M, Marinkovic K (1994a) Spatio-temporal stages in face and word processing. 1. Depth recorded potentials in the human occipital and parietal lobes. J Physiology Paris 88:1–50.

Halgren E, Baudena P, Heit G, Clarke M, Marinkovic K, Chauvel P (1994b) Spatio-temporal stages in face and word processing. 2. Depth-recorded potentials in the human frontal and Rolandic cortices. J Physiology Paris 88:51–80.

Halgren E, Dhond RP, Christensen N, Van Petten C, Marinkovic K, Lewine JD (2002): N400-like magnetoencephalography responses modulated by semantic context, word frequency, and lexical class in sentences. Neuroimage 17:1101–1116.

Hanslmayr S, Klimesch W, Sauseng P, Gruber W, Doppelmayr M, Freunberger R, Pecherstorfer T, Birbaumer N (2007): Alpha phase reset contributes to the generation of ERPs. Cerebral Cortex 17:1–8.

Helenius P, Salmelin R, Richardson U, Leinonen S, Lyytinen H (2002): Abnormal auditory cortical activation in dyslexia 100 msec after speech onset. J Cogn Neurosci 14:603–617.

Helenius P, Salmelin R, Service E, Connolly JF (1998): Distinct time courses of word and context comprehension in the left temporal cortex. Brain 121:1133–1142.

Hirata M, Kato A, Taniguchi M, Saitoh Y, Ninomiya H, Ihara A, Kishima H, Oshino S, Baba T, Yorifuji S, Yoshimine T (2004): Determination of language dominance with synthetic aperture magnetometry: Comparison with the Wada test. Neuroimage 23:46–53.

Hirata M, Koreeda S, Sakihara K, Kato A, Yoshimine T, Yorifuji S (2007): Effects of the emotional connotations in words on the frontal areas—A spatially filtered MEG study. Neuroimage 35:420–429.

Hämäläinen M (2009): MNE Software. User's Guide. MGH/HMS/MIT Athinoula A. Martinos Center for Biomedical Imaging, Charlestown, MA, USA.

Hämäläinen M, Hari R, Ilmoniemi RJ, Knuutila J, Lounasmaa OV (1993): Magnetoencephalography—Theory, instrumentation, and applications to noninvasive studies of the working human brain. Rev Mod Phys 6:413–497.

Hämäläinen M, Ilmoniemi R (1994): Interpreting magnetic fields of the brain: Minimum norm estimates. Med Biol Eng Comput 32:35–42.

Intriligator J, Polich J (1994): On the relationship between background EEG and the P300 event-related potential. Biol Psychol 37:207–218.

Jasiukaitis P, Hakerem G (1988): The effect of prestimulus alpha activity on the P300. Psychophysiology 25:157–165.

Kaiser J, Birbaumer N, Lutzenberger W (2001): Event-related beta desynchronization indicates timing of response selection in a delayed-response paradigm in humans. Neurosci Lett 312:149–152.

Karrasch M, Laine M, Rapinoja P, Krause CM (2004): Effects of normal aging on event-related desynchronization/synchronization during a memory task in humans. Neurosci Lett 366:18–23.

Kim JS, Chung CK (2008): Language lateralization using MEG beta frequency desynchronization during auditory oddball stimulation with one-syllable words. NeuroImage 42:1499–1507.

Klimesch W (1999): EEG alpha and theta oscillations reflect cognitive and memory performance: A review and analysis. Brain Res Rev 29:169–195.

Klimesch W, Doppelmayr M, Pachinger T, Ripper B (1997a) Brain oscillations and human memory: EEG correlates in the upper alpha and theta band. Neurosci Lett 238:9–12.

Klimesch W, Doppelmayr M, Pachinger T, Russegger H (1997b) Event-related desynchronization in the alpha band and the processing of semantic information. Cogn Brain Res 6:83–94.

Klimesch W, Neuper C (2006): Oscillatory Brain Dynamics During Language Comprehension. Amsterdam: The Netherlands, Elsevier.

Kutas M, Federmeier K (2000): Electrophysiology reveals semantic memory use in language comprehension. Trends Cogn Sci 4:436–470.

Kutas M, Federmeier KD (2011): Thirty years and counting: finding meaning in the N400 component of the event-related brain potential (ERP). Annu Rev Psychol 62:621–647.

Lau EF, Phillips C, Poeppel D (2008): A cortical network for semantics: (de)constructing the N400. Nat Rev Neurosci 9:920–933.

Liu X, Qi H, Wang S, Wan M (2006): Wavelet-based estimation of EEG coherence during Chinese Stroop task. Comput Biol Med 36:1303–1315.

Maris E, Oostenveld R (2007): Nonparametric statistical testing of EEG- and MEG-data. J Neurosci Methods 164:177–190.

Makeig S, Debener S, Onton J, Delorme A (2004): Mining event-related brain dynamics. Trends Cogn Sci 8:204–210.

Makeig S, Westerfield M, Jung T-P, Enghoff S, Townsend J, Courchesne E, Sejnowski TJ (2002): Dynamic brain sources of visual evoked responses. Science 295:690–694.

Mäkinen V, Tiitinen H, May P (2005): Auditory event-related responses are generated independently of ongoing brain activity. NeuroImage 24:961–968.

Mathewson KE, Gratton G, Fabiani M, Beck DM, Ro T (2009): To see or not to see: Prestimulus alpha phase predicts visual awareness. J Neurosci 29:2725–2732.

Mazaheri A, Picton TW (2005): EEG spectral dynamics during discrimination of auditory and visual targets. Cogn Brain Res 24:81–96.

McCarthy G, Nobre AC, Bentin S, Spencer DD (1995): Language-related field potentials in the anterior-medial temporal lobe: I. Intracranial distribution and neural generators. J Neurosci 15:1080–1089.

Nobre A, McCarthy G (1995): Language-related field potentials in the anterior-medial temporal lobe: II. Effects of word type and semantic priming. J Neurosci 15:1090–1098.

Nolte G (2003): The magnetic lead field theorem in the quasi-static approximation and its use for magnetoencephalography forward calculation in realistic volume conductors. Phys Med Biol 48:3637–3652.

Oostenveld R, Fries P, Maris E, Schoffelen JM (2011): Field trip: Open source software for advanced analysis of MEG, EEG, and invasive electrophysiological data. Comput Intell Neurosci 156869.

Parkes LM, Bastiaansen MCM, Norris DG (2006): Combining EEG and fMRI to investigate the post-movement beta rebound. Neuroimage 29:685–696.

Pesonen M, Bjornberg CH, Hamalainen H, Krause CM (2006): Brain oscillatory 1–30 Hz EEG ERD/ERS responses during the different stages of an auditory memory search task. Neurosci Lett 399:45–50.

Peterson DA, Thaut MH (2002): Delay modulates spectral correlates in the human EEG of non-verbal auditory working memory. Neurosci Lett 328:17–20.

Pfurtscheller G, Lopes da Silva FH (1999): Event-related EEG-MEG synchronization and desynchronization: Basic principles. Clin Neurophysiol 110:1842–1857.

Pfurtscheller G, Stancák A, Jr, Neuper C (1996): Post-movement beta synchronization: A correlate of an idling motor area? Electroencephalogr Clin Neurophysiol 98:281–293.

Pfurtscheller G, Zalaudek K, Neuper C (1998): Event-related beta synchronization after wrist, finger and thumb movement. Electroencephalogr Clin Neurophysiol/Electromyogr Motor Control 109:154–160.

Rohm D, Klimesch W, Haider H, Doppelmayr M (2001): The role of theta and alpha oscillations for language comprehension in the human electroencephalogram. Neurosci Lett 310:137–140.

Salmelin RH, Hämäläinen MS (1995): Dipole modeling of MEG rhythms in time and frequency domains. Brain Topogr 7:251–257.

Salmelin R, Service E, Kiesila P, Uutela K, Salonen O (1996): Impaired visual word processing in dyslexia revealed with magnetoencephalography. Ann Neurol 40:157–162.

Schack B, Chen ACN, Mescha S, Witte H (1999): Instantaneous EEG coherence analysis during the Stroop task. Clin Neurophysiol 110:1410–1426.

Shah AS, Bressler SL, Knuth KH, Ding M, Mehta AD, Ulbert I, Schroeder CE (2004): Neural dynamics and the fundamental mechanisms of event-related brain potentials. Cereb Cortex 14:476–483.

Sheth BR, Sandkd́uhler S, Bhattacharya J (2009): Posterior beta and anterior gamma oscillations predict cognitive insight. J Cogn Neurosci 21:1269–1279.

Sinkkonen J, Tiitinen H, Näatänen R (1995): Gabor filters: An informative way for analysing event-related brain activity. J Neurosci Methods 56:99–104.

Snijders TM, Petersson KM, Hagoort P (2010): Effective connectivity of cortical and subcortical regions during unification of sentence structure. NeuroImage 52:1633–1644.

Stancák A Jr, Pfurtscheller G (1996): Event-related desynchronisation of central beta-rhythms during brisk and slow self-paced finger movements of dominant and nondominant hand. Cogn Brain Res 4:171–183.

Supp GG, Schlögl A, Gunter TC, Bernard M, Pfurtscheller G, Petsche H (2004): Lexical memory search during N400: Cortical couplings in auditory comprehension. NeuroReport 15:1209–1213.

Tallon-Baudry C (2003): Oscillatory synchrony and human visual cognition. J Physiol (Paris) 97:355–363.

Tallon-Baudry C, Bertrand O (1999): Oscillatory gamma activity in humans and its role in object representation. Trends Cogn Sci 3:151–162.

Tallon-Baudry C, Bertrand O, Delpuech C, Pernier J (1996): Stimulus specificity of phase-locked and non-phase-locked 40 Hz visual responses in human. J Neurosci 16:4240–4249.

van den Brink D, Brown CM, Hagoort P (2001): Electrophysiological evidence for early contextual influences during spoken-word recognition: N200 versus N400 effects. J Cogn Neurosci 13:967–985.

Vartiainen J, Parviainen T, Salmelin R (2009): Spatiotemporal convergence of semantic processing in reading and speech perception. J Neurosci 29:9271–9280.

Weiss S, Mueller HM (2003): The contribution of EEG coherence to the investigation of language. Brain Lang 85:325–343.

Weiss S, Mueller HM, Schack B, King JW, Rappelsberger P (2005): Increased neuronal communication accompanying sentence comprehension. Int J Psychophysiol 57:129–141.

Xiang H-D, Fonteijn HM, Norris DG, Hagoort P (2010): Topographical functional connectivity pattern in the perisylvian language networks. Cereb Cortex 20:549–560.

Yamamoto M, Ukai S, Shinosaki K, Ishii R, Kawaguchi S, Ogawa A, Mizuno-Matsumoto Y, Fujita N, Yoshimine T, Takeda M (2006): Spatially filtered Magnetoencephalographic analysis of cortical oscillatory changes in basic brain rhythms during the Japanese "Shiritori" word generation task. Neuropsychobiology 53:215–222.